Experimental investigation of nanosecond discharge plasma aerodynamic actuation*

Wu Yun(吴 云)†, Li Ying-Hong(李应红), Jia Min(贾 敏), Liang Hua(梁 华), and Song Hui-Min(宋慧敏)

Science and Technology on Plasma Dynamics Laboratory, Air Force Engineering University, Xi'an 710038, China

(Received 15 June 2011; revised manuscript received 6 September 2011)

In this paper we report on an experimental study of the characteristics of nanosecond pulsed discharge plasma aerodynamic actuation. The N_2 ($C^3\Pi_u$) rotational and vibrational temperatures are around 430 K and 0.24 eV, respectively. The emission intensity ratio between the first negative system and the second positive system of N_2, as a rough indicator of the temporally and spatially averaged electron energy, has a minor dependence on applied voltage amplitude. The induced flow direction is not parallel, but vertical to the dielectric layer surface, as shown by measurements of body force, velocity, and vorticity. Nanosecond discharge plasma aerodynamic actuation is effective in airfoil flow separation control at freestream speeds up to 100 m/s.

Keywords: plasma aerodynamic actuation, nanosecond pulsed discharge, plasma flow control, optical emission spectra

PACS: 52.50.Dg, 52.80.Pi, 52.70.Kz, 47.85.L– **DOI:** 10.1088/1674-1056/21/4/045202

1. Introduction

Plasma flow control, based on the plasma aerodynamic actuation generated by air discharge, is a novel flow control method to improve aerodynamic characteristics and propulsion efficiency.[1−8] The mechanism for plasma flow control can be summarized as momentum effect, shock effect, and chemical effect. Momentum effect induces a near-surface flow velocity of 1 m/s–6 m/s,[2,3] shock effect induces local gas pressure or temperature rise near the electrode, and chemical effect adds new particles, such as ions, electrons, and excited particles, into the flow field.

Most of the previous experimental and simulation studies mainly focused on asymmetric dielectric barrier discharge plasma aerodynamic actuation excited by sinusoidal or sawtooth voltage waveforms with amplitudes in a range of 2 kV–20 kV and frequencies in a range of 1 kHz–100 kHz, which can be named microsecond discharge plasma aerodynamic actuation.[1−7] It is widely recognized that momentum effect, which induces boundary layer acceleration, is the main mechanism for microsecond discharge plasma aerodynamic actuation in low speed (0.1 Mach–0.2 Mach) flow separation control.[1,2] Recent experimental results have indicated that nanosecond discharge plasma aerodynamic actuation is still effective at 0.85 Mach.[8] Since the induced velocity is very tiny,[8] the mechanism for nanosecond discharge plasma flow control may not be momentum-effect.

In order to better understand the underlying physical mechanism of nanosecond discharge plasma flow control, it is important to investigate the characteristics of nanosecond discharge plasma aerodynamic actuation. Discharge propagation, reduced electric field, the pressure in the plasma layer, induced flow velocity, and the gasdynamic perturbations of a nanosecond discharge plasma aerodynamic actuator were experimentally studied in Ref. [8]. A physical model for the plasma aerodynamic actuator excited by repetitive nanosecond voltage pulses was developed in Ref. [9]. The plasma aerodynamic actuator driven by repetitive nanosecond voltage pulses with DC or low frequency sinusoidal bias was experimentally studied in Ref. [10]. The voltage distribution in a nanosecond discharge plasma aerodynamic actuator of 2.4 m in length was numerically and experimentally studied in Ref. [11]. A two-dimensional self-consistent numerical model of the nanosecond discharge plasma aerodynamic actu-

*Project supported by the National Natural Science Foundation of China (Grant Nos. 50906100 and 10972236) and the Science Foundation of National Excellent Doctoral Dissertation of China (Grant No. 201172).

†Corresponding author. E-mail: wuyun1223@126.com

© 2012 Chinese Physical Society and IOP Publishing Ltd

ator was developed in Ref. [12], and the mechanism of ultra-fast heating in nanosecond surface discharge plasma was investigated in Ref. [13]. In this paper, we report on an experimental study of the characteristics of nanosecond discharge plasma aerodynamic actuation at one atmosphere.

2. Experimental setup

A schematic plot of the dielectric barrier discharge plasma aerodynamic actuator is shown in Fig. 1. The dielectric layer used is an RO4350B (Rogers Corporation) plate with a relative permittivity constant of 3.48. The electrodes are made of copper, covered with lead-tin film. The lower electrode, which is covered with silica gel, is grounded. The output voltage and the frequency range of the power supply are 5 kV–80 kV and 0.1 kHz–2 kHz, respectively.

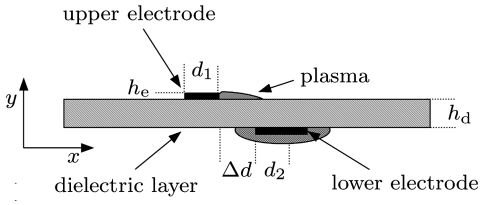


Fig. 1. A schematic diagram of the asymmetric surface dielectric barrier discharge plasma aerodynamic actuator. d_1, d_2, Δd, h_d, and h_e are 2 mm, 3 mm, 1 mm, 0.5 mm, and 0.035 mm respectively. The span length is 100 mm.

The applied voltage and discharge current are measured by a high voltage probe (Tektronix P6015A) and a current probe (Tektronix TCP312+TCPA300), respectively. Signals are recorded on an oscilloscope (Tektronix DPO4104). Optical emission spectra are obtained using a charge coupled device spectrometer (Avantes 2048) through an optical fiber, located 1 mm above the surface of the dielectric layer and 1 mm downstream of the upper electrode. The exposure time is 1 s. The emission intensity is averaged temporally and spatially. The optical emission experiments are performed in a dark room, and the background noise is measured before each test and subtracted during post-processing. The body force induced by plasma aerodynamic actuation is measured by an electronic balance (Mettler Toledo ABS 204-S), and the resolution of the electronic balance (Mettler Toledo ABS 204-S) is 10^{-6} N. The force measurement is made by mounting an actuator on a stand. A 32AWG wire is used to connect the power supply and the actuator in order to limit spring forces to a negligible level. The balance is held in a grounded copper mesh to eliminate RF interference, and the accuracy of the balance measurements is 5%. The velocity and vorticity induced by the plasma aerodynamic actuation are measured by particle image velocimetry (PIV) (Lavision). The PIV set-up consists of a Litron double-pulsed Nd:YAG laser system as the light source and a Lavision ProX 2M camera to record the images. The camera is operated in shuttered mode at 30 Hz frame rate with a single image exposure time of 1 ms. The air is seeded by vaporization of mineral oil with a mean size of about 0.3 μm. The measurement error is 0.1 m/s.

3. Results and discussion

Figure 2 shows the applied voltage and discharge current traces of the nanosecond discharge. The voltage pulse has an FWHM of 190 ns and a rise time of 450 ns. The driving frequency is 1 kHz.

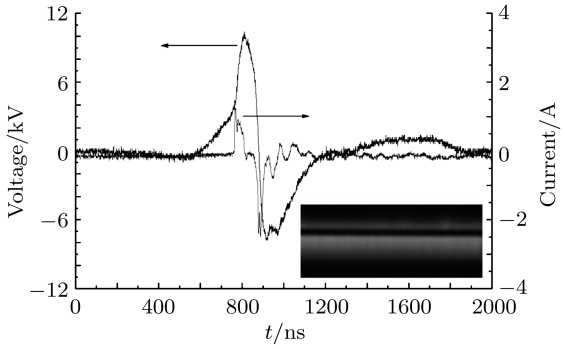


Fig. 2. Traces of the applied voltage and discharge current. The inset shows the uniform atmospheric air plasma.

Though the applied voltage is a unipolar positive pulse, positive current pulses and negative current pulses are observed. The positive current pulses are produced as the applied voltage exceeds the breakdown voltage of the gas, while the negative current pulses represent discharge occurring on the falling edge of the voltage pulse.[14] With an applied pulse amplitude of 10 kV, the discharge current is of the order of 2.5 A, which is significantly different from the discharge current in the microsecond discharge plasma with an amplitude typically of the order of tens to hundreds of milliamperes.[2] Thus the peak dissipated power in nanosecond discharge plasma aerodynamic actuation is much higher than that in microsecond discharge plasma aerodynamic actuation, which is beneficial for plasma flow control. The discharge is visibly diffused even when the inner gap of an electrode

pair (Δd) is 1 mm, which is significantly different from the filamentary discharge in the microsecond discharge plasma, as shown in Fig. 3.[15]

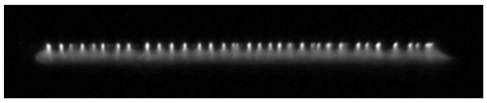


Fig. 3. Filamentary discharge in microsecond discharge plasma ($\Delta d = 1$ mm).

The optical emission spectrum of the nanosecond discharge plasma is shown in Fig. 4. The applied voltage and driving frequency are 10 kV and 1 kHz, respectively. The major spectra come from the second positive system (SPS) of $N_2(C^3\Pi_u \rightarrow B^3\Pi_g)$ and the first negative system (FNS) of $N_2^+(B^2\Sigma_u^+ \rightarrow X^2\Sigma_g^+)$.

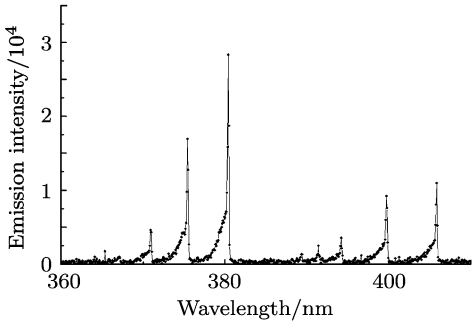


Fig. 4. The optical emission spectrum of the nanosecond discharge plasma.

The gas temperature is close to the rotational temperature because rotational relaxation is fast at atmospheric pressure. The rotational temperature of N_2 is obtained by fitting the measured profile of the emission band near 380.5 nm to the simulated one, while the vibrational temperature is calculated with the intensity ratio between the spectral lines at 371.1 nm and 380.5 nm.[16] When the upper electrode is powered, the rotational and the vibrational temperatures of N_2 are 430 K and 0.25 eV, respectively.

The intensity ratio between the spectral lines from FNS and SPS is strongly dependent on the average electron energy and electron energy distribution function (EEDF), because the excited thresholds of the two processes have a difference of about 8 eV, as shown in Ref. [17]. Here, we use the intensity ratio between spectral lines at 391.4 nm from FNS and 380.5 nm from SPS ($I_{391.4}/I_{380.5}$) as a rough indicator of the temporally and spatially averaged electron energy. When the applied voltage is 10 kV, $I_{391.4}/I_{380.5}$ is 0.08 in the nanosecond discharge plasma. The experimental uncertainty is estimated to be 5%, with the instrument error and the experimental error taken into account. In the nanosecond discharge plasma the maximum instantaneous electron energy is much higher than that in the microsecond discharge plasma.[18] Because of the frequent collisions at one atmosphere, electrons with higher energy decay faster. Thus, the emission intensity of 391.4 nm drops off much faster than that of 380.5 nm, which is a possible reason for such a small value of the temporally and spatially averaged intensity ratio between spectral lines at 391.4 nm and 380.5 nm. The rotational temperature remains around 430 K($\pm$30 K) when the voltage increases from 8 kV to 12 kV.

The intensity ratios between spectral lines at 391.4 nm and 380.5 nm, and between those at 371.1 nm and 380.5 nm versus applied voltage are shown in Fig. 5. It can be concluded that the temporally and spatially averaged electron energy and vibrational temperature have minor dependences on applied voltage amplitude. The reason for this may be that the frequent collisions between electrons and molecules govern the discharge process at one atmosphere. The collision-less free path of the electrons, 70 nm–90 nm, mainly determines the energy obtained by the electron from the electric field.

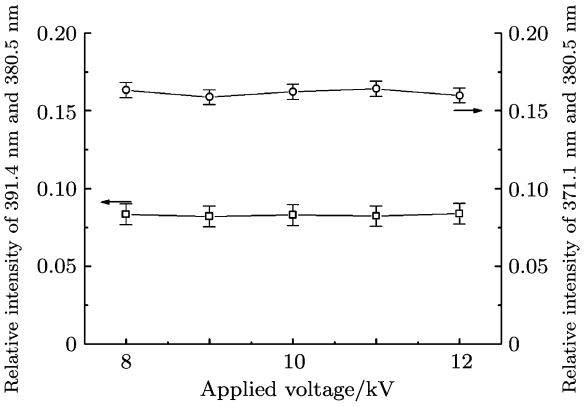


Fig. 5. Relative emission intensities versus applied voltage.

The induced body forces in the x direction and the y direction versus applied voltage are shown in Fig. 6. The induced body force is almost zero in the x direction, while it is about 15 mN in the y direction. The body force per unit length of electrode is of the order of 3 mN per cm in the y direction. It is inferred that the induced flow direction is vertical to the dielectric layer surface, while the flow induced by

microsecond discharge plasma aerodynamic actuation is parallel to the dielectric layer surface.[2]

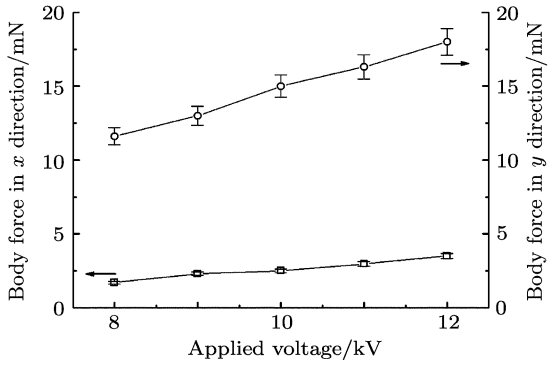


Fig. 6. Induced body forces versus applied voltage.

This result is confirmed in the velocity and vorticity measurements by the PIV, and shown in Fig. 7. The flow direction is almost vertical to the dielectric layer surface, which corresponds to the body force measurement result. The velocity field is measured during discharge 2 s after the actuator has switched on.

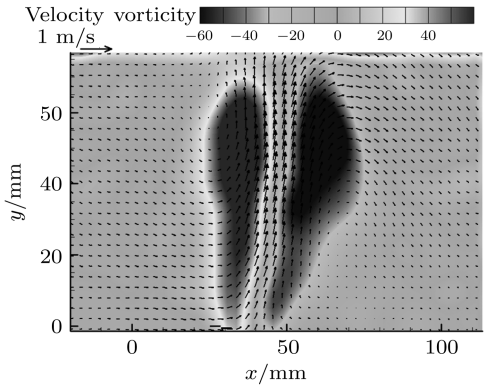


Fig. 7. Velocity and vorticity induced by nanosecond discharge plasma aerodynamic actuation (2 s after the actuator has switched on).

Fast heating may be the reason for the vertical motion of air near the electrode, as shown in Refs. [12] and [13]. Due to the fast heating, a shock wave, which rises several microseconds after the actuator has switched on and disperses into weak disturbance after tens to hundreds of microseconds, can be taken by a high speed shadowgraph.[8] In this paper, due to the low frequency response of electronic balance and PIV, only the slow vertical motion or weak disturbance can be monitored. Thus, the flow control mechanism for nanosecond discharge plasma aerodynamic actuation is presumed to be thermal shock effect, which induces local pressure or temperature rise near the electrode. In other words, this is a different sort of momentum transfer mechanism, other than the momentum transfer due to charged particle acceleration in an electric field. The air motion is caused by chaotic collisions of heated neutral particles in an upward direction due to gas heating.

Flow separation control experiments are carried out in a wind tunnel to validate the performance of nanosecond discharge plasma aerodynamic actuation. An NACA 0015 airfoil, of which the chord length is 120 mm, is used in the experiment. Pressure sensors are located at 8%, 15%, 35%, 40%, 60%, and 80% of the chord length, respectively. The plasma aerodynamic actuator used in the present experiment consists of 3 electrode pairs, located at 2%, 20%, and 45% of the chord length, respectively. The electrodes are parallel to the leading edge of the blade. With nanosecond discharge plasma aerodynamic actuation at a freestream velocity of 100 m/s (corresponding Re is 9.2×10^5), the critical stall angle increases from 22° to 25°, and when the angle is 22°, the lift calculated from the pressure distribution increases by 17.4%, which is shown in Figs. 8 and 9. The horizontal axis is the relative location to the chord length of the airfoil. Compared with the strength of microsecond discharge plasma aerodynamic actuation, the strength of nanosecond discharge plasma aerodynamic actuation is very strong due to the thermal shock effect. This vertical actuation caused by thermal shock effect can also induce many more vortexes near the surface in high speed flow, while the boundary layer acceleration caused by the conventional momentum effect becomes very weak at this time. Thus, nanosecond discharge plasma aerodynamic actuation is very suitable for high speed flow separation control.

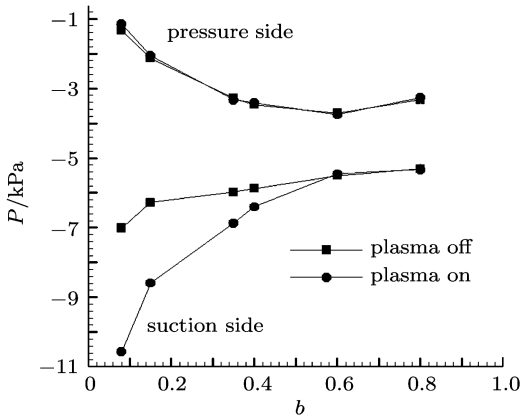


Fig. 8. Pressure distribution on the suction and pressure surfaces of the NACA 0015 airfoil, with the freestream velocity and angle of attack being 100 m/s and 22°, respectively.

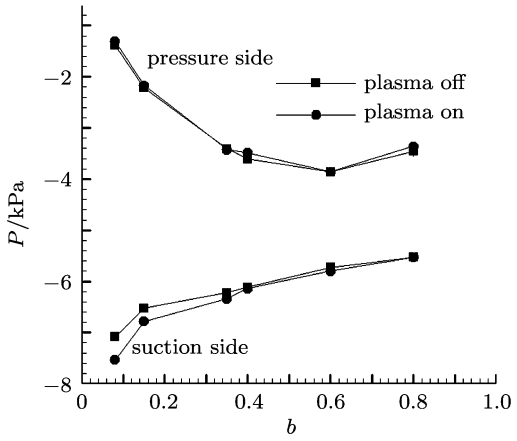


Fig. 9. Pressure distribution on the suction and pressure surfaces of the NACA 0015 airfoil, with the freestream velocity and angle of attack being 100 m/s and 25°, respectively.

4. Conclusion

The characteristics of nanosecond discharge plasma aerodynamic actuation are different from those of conventional microsecond discharge plasma aerodynamic actuation. The peak power in nanosecond discharge plasma is much higher. The $N_2(C^3\Pi_u)$ rotational and vibrational temperatures are around 430 K and 0.24 eV, respectively. The emission intensity ratio between the first negative system and the second positive system of N_2 has a minor dependence on applied voltage amplitude, and the induced flow direction is vertical but not parallel to the dielectric layer surface, which may be caused by the thermal shock effect during the discharge near the electrode. Nanosecond discharge plasma aerodynamic actuation is effective in airfoil flow separation control at a freestream speed of up to 100 m/s, which is much more effective than conventional microsecond discharge plasma aerodynamic actuation.

Acknowledgements

The authors thank Zhang Shu, Wan Jun, Chen Wen-Cong, and Ma Qing-Yuan for the help in the experiment and analysis.

References

[1] Corke T C, Post M L and Orlov D M 2010 *Prog. Aerospace Sci.* **43** 505
[2] Moreau E 2007 *J. Phys.* D: *Appl. Phys.* **40** 605
[3] Roth J R 2003 *Phys. Plasmas* **10** 2117
[4] Enloe C L, McLaughlin T E, Dyken R D V and Kachner K D 2004 *AIAA J.* **42** 589
[5] Wu Y, Li Y H, Jia M, Song H M, Guo Z G, Zhu X M and Pu Y K 2008 *Appl. Phys. Lett.* **93** 031503
[6] Pinheiro M J 2006 *Plasma Process. Polym.* **3** 135
[7] Li Y H, Wu Y, Zhou M, Su C B, Zhang X W and Zhu J Q 2010 *Exp. Fluids* **48** 1015
[8] Roupassov D V, Nikipelov A A, Nudnova M M and Starikovskii A Y 2009 *AIAA J.* **47** 168
[9] Likhanskii A V, Shneider M N, Macheret S O and Miles R B 2007 *Phys. Plasmas* **14** 073501
[10] Opaits D F, Likhanskii A V, Neretti G, Zaidi S, Shneider M N, Miles R B and Macheret S O 2008 *J. Appl. Phys.* **104** 043304
[11] Opaits D F, Shneider M N and Miles R B 2009 *Appl. Phys. Lett.* **94** 061503
[12] Unfer T and Boeuf J P 2009 *J. Phys.* D: *Appl. Phys.* **42** 194017
[13] Aleksandrov N L, Kindysheva S V, Nudnova M M and Starikovskiy A Y 2010 *J. Phys.* D: *Appl. Phys.* **43** 255201
[14] Walsh J L and Kong M G 2007 *Appl. Phys. Lett.* **91** 251504
[15] Li Y H, Wu Y, Jia M, Zhou Z W, Guo Z G and Pu Y K 2008 *Chin. Phys. Lett.* **25** 4068
[16] Wu Y, Li Y H, Jia M, Song H M, Su C B and Pu Y K 2010 *Chin. J. Aeronaut.* **23** 39
[17] Choi J H, Lee T I, Han I, Baik H K, Song K M, Lim Y S and Lee E S 2006 *Plasma Sources Sci. Technol.* **15** 416
[18] Macheret S O, Shneider M N and Miles R B 2002 *IEEE Trans. Plasma Sci.* **30** 1301